THE JOURNAL OF PHYSICAL CHEMISTRY B

ARTICLE

pubs.acs.org/JPCB

Two Glass Transitions and Secondary Relaxations of Methyltetrahydrofuran in a Binary Mixture

T. Blochowicz,*[,†] S. A. Lusceac,[†] P. Gutfreund,[‡] S. Schramm,[†] and B. Stühn[†]

[†]Institut für Festkörperphysik, TU-Darmstadt, 64289 Darmstadt, Germany

[‡]Institut Laue-Langevin, 38042 Grenoble Cedex, France

ABSTRACT: We investigate the molecular dynamics in the binary glass forming system methyltetrahydrofuran (M-THF) and tristyrene. Although the components are miscible in the full concentration and temperature range, two glass transitions can clearly be distinguished in differential scanning calorimetry. We selectively probe the reorientational dynamics of M-THF and tristyrene by means of dielectric spectroscopy and depolarized dynamic light scattering, respectively. While, apart from the observed plasticizer effect, the motion of the larger molecules remains almost unchanged, it is shown that the smaller M-THF molecules take part in both glass transitions. Moreover, below the upper T_g of the mixture, the remaining mobile M-THF molecules clearly show confinement effects in their relaxation behavior. In order to elucidate the nature of the observed secondary relaxation processes, we first characterize the influence of the methyl group of M-THF on the dynamics in the mixtures by comparing the results obtained so far with the relaxation behavior observed in blends of THF and tristyrene. Finally, we employ ^{2}H NMR spectroscopy to clarify the nature of the secondary relaxations of THF-d_8 in the latter mixtures and conclude on the basis of the NMR and dielectric results that the high-frequency wing observed in neat M-THF appears as a genuine Johari−Goldstein β-relaxation in the mixtures, whereas the faster secondary process is due to internal degrees of freedom of the nonrigid THF ring.

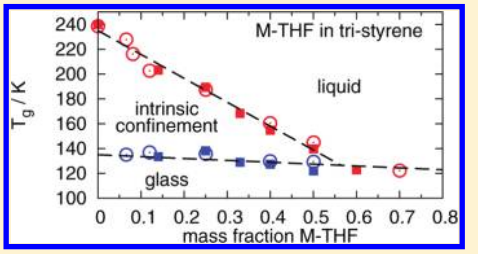

INTRODUCTION

The glass transition in binary liquids recently has become a field of intense research, not only because of the broad range of applications that become available when tailoring material properties by blending[1] but also due to the rather peculiar and complex features that are observed in the molecular dynamics of these blends.[2,3]

Pronounced dynamic heterogeneities are among the most important dynamical properties in the relaxation of binary systems. They are observed as broadening of relaxation time distributions compared to the relaxation of the neat bulk materials, and often violations of the time−temperature superposition principle are reported.[3] In the case of dynamically very asymmetric mixtures, i.e., in mixtures with a high T_g contrast of the components, even a decoupling of the dynamics of host and guest molecules is observed, as small molecules may undergo isotropic reorientation even far below the average glass transition temperature T_g of the mixture.[2,4,5] Thus, contrary to the traditional notion that identifies macroscopic miscibility with a single glass transition step,[1] two glass transitions were recently reported in well-miscible polymer blends,[6−9] polymer solutions, and polymer plasticizer systems.[10−14] And also in mixtures of small organic molecules, a decoupling in the dynamics of both components is observed, e.g., by calorimetry, and dielectric and nuclear magnetic resonance spectroscopy.[2,15,16]

Often, this kind of dynamic heterogeneity is explained in terms of local concentration variations, which are attributed to either thermally driven concentration fluctuations[17−19] or so-called self-concentration effects due to chain connectivity in polymers,[20,21] or a combination of both mechanisms.[22,23] In the case of low molecular weight binary mixtures, concentration fluctuations are expected to play the dominating role and could also lead to a separation of time scales,[18] but recently it was suggested that self-concentration effects might also be important in low molecular weight systems due to a different cooperative volume relevant for the relaxation of each component.[24] We also note, however, that in athermal polymer/oligomer blends so far a separation of time scales has not directly become evident, at least from calorimetric studies[25,26] and that the self-concentration model was found to at least overestimate the separation of time scales in these mixtures.[27]

An entirely different view on the dynamics in binary systems is presented in the framework of mode coupling theory (MCT), where a dynamic decoupling of large and small particles is anticipated, if the components differ enough in size.[28−30] In that case, the smaller particles retain mobility below the glass transition of the larger ones and undergo a localization transition in the confinement of a frozen matrix. This scenario was recently confirmed by simulations.[31] Thus, confinement effects are indeed expected in a certain temperature interval in binary mixtures[3]

Received: November 3, 2010
Revised: December 14, 2010
Published: February 2, 2011

and therefore recent theoretical work on MCT in so-called quenched−annealed systems[32−34] and simulations for a Lorentz-gas model[35] might also be relevant for binary mixtures. In particular, it is interesting to note that in such systems MCT predicts higher order singularities[34] in the vicinity of which the correlation functions of the smaller molecules become particularly broad and logarithmic decay curves are observed in simulations[36] and experiments.[5]

Another aspect of the broadening of relaxation processes observed in binary mixtures is the fact that different relaxational contributions in the spectra of the small molecules can be separated when the latter are mixed with a considerably slower matrix.[37,38] For example, in mixtures of 2-picoline and oligostyrene it was observed that the high-frequency wing of picoline turns out to be a Johari−Goldstein (JG) β-relaxation, when the α-process is sufficiently slowed down in a binary mixture.[37] Thus, the high-frequency wing was clearly shown not to be a part of the α-relaxation. Of course, the question arises whether this finding can be reproduced for solvent molecules that show a secondary relaxation besides a clearly discernible high-frequency wing, as it was reported, e.g., for methyltetrahydrofuran (M-THF).[39] Thus, the binary mixture M-THF in tristyrene investigated in the present paper was not only chosen because of the miscibility and the large T_g contrast of 149 K, but also due to the fact that two secondary relaxations are present in M-THF, the nature of which is not yet clarified. Moreover, this particular mixture shows a large contrast in the electric dipole moment and in the optical anisotropy, such that the molecular reorientation of M-THF is selectively monitored by dielectric spectroscopy, whereas depolarized dynamic light scattering is at the same time able to probe the reorientational correlation function of tristyrene. In addition, we will try to clarify the nature of the appearing secondary relaxations by applying ^{2}H NMR to mixtures of THF in tristyrene, as both mixtures turn out to be hardly different from a dynamical point of view.

The paper is organized as follows: after a short introduction of the experimental procedures and techniques that are used in the course of this investigation, we briefly introduce our approach for analyzing the dielectric and dynamic light scattering data. Then, we present our results obtained for the mixtures of M-THF and tristyrene by means of differential scanning calorimetry (DSC), dielectric spectroscopy (DS) and depolarized dynamic light scattering (DDLS). Here, we particularly emphasize the dynamic decoupling effects observed in the α-relaxations of the components in the blend. Finally, we focus on the observed secondary relaxations by comparing the results obtained in M-THF/tristyrene mixtures with the relaxation behavior of THF/tristyrene blends. The latter are investigated by DS to show that both are indeed very similar and finally by ^{2}H NMR, which helps to clarify the underlying motional mechanisms of the secondary relaxations.

MATERIALS AND METHODS

Tristyrene was purchased from Polymer Standards Service (Mainz, Germany) and used without further purification. Tristyrene was available as a distilled sample, so that the oligomer is monodisperse and ionic impurities, which cause the dc-conductivity contribution in dielectric spectroscopy, are greatly reduced.

Protonated THF and M-THF were obtained from Acros Organics. M-THF was purchased as extra-dry sample and used as received whereas THF was double-distilled prior to usage. For the NMR experiments tetrahydrofuran-d_8 (99.5% deuteration) was purchased from Sigma-Aldrich and used as received. As THF and M-THF both are very volatile substances, care had to be taken to ensure a well-defined concentration of the solvent in the mixtures during preparation and transfer of the material into the respective sample cells. Thereafter, the weight of the filled cells was monitored over a fixed period of time to make sure that the cells were sealed and a well-defined solvent concentration was obtained in the course of the experiment.

Differential scanning calorimetry measurements were performed using a DSC Q-1000 from TA-Instruments with liquid nitrogen cooling, which provides sufficient baseline stability and resolution down to 100 K. For each measurement, about 10 mg of sample was equilibrated at 313 K for 3 min, cooled down to 95 K, and after an equilibration time of another 3 min heated up again to 300 K. Always the same rate was chosen for heating and cooling in each run. All DSC results shown in this work are the ones acquired while heating.

The dielectric measurements were performed in the frequency domain using a Novocontrol Alpha-N High Resolution Dielectric Analyzer in the frequency range from 10^{-4} to 10^7 Hz. The sample was contained in a spacer-free, O-ring-sealed parallel plate capacitor (diameter 18 mm, gap 50 μm). The temperature was controlled using a nitrogen gas cryostat (Novocontrol Quattro) with an absolute accuracy of $\pm$0.5 K.

The ^{2}H NMR experiments were carried out using a home-built probe and spectrometer together with an Oxford superconducting magnet operating at a field of about 7 T corresponding to a ^{2}H Larmor frequency of ν_0 = 46.2 MHz. The probe was placed in a continuous-flow cryostat (CryoVac) operated with liquid nitrogen and controlled by a CryoVac TIC 304 MA temperature controller. The long-time temperature stability was better than $\pm$0.5 K. For spectra acquisition, we used a solid-echo pulse sequence[40] preceded by a saturation sequence. The solid-echo sequence consists of two $\pi/2$ pulses shifted in phase by 90° and separated by a time period t_p: $(\pi/2)_x-t_p-(\pi/2)_y$. A $\pi/2$ pulse length of 2.2 μs was attainable ensuring the excitation of the broad deuteron spectrum; the time t_p was set to 25 μs. The delay after the saturation sequence was chosen to probe more than 95% of the equilibrium magnetization. In order to obtain the spin−lattice relaxation time, we employed the same pulse sequence, namely a saturation sequence followed by a solid-echo pulse sequence, in this case at variable waiting times.

Photon correlation spectroscopy (PCS) was performed in both polarized (vv) and depolarized (vh) scattering geometry using a standard PCS setup from ALV, Langen, Germany, including goniometer and a 5000E hardware correlator card in combination with a CryoVac optical coldfinger cryostat. The cylindrical sample cell was illuminated by a focused and polarized 25 mW He−Ne laser beam. The scattered light first passed through a Glan-Thompson polarizer to define the scattering geometry and was then coupled into an optical fiber mounted on the goniometer. Finally, the photon counting was done either by means of a single avalanche photodiode, typically in vh-geometry for count rates <10 kHz, or, in vv-geometry at sufficiently high countrates by an ALV dual photo detection unit (ALV/SO-SIPD) in pseudo-cross-correlation mode in order to suppress afterpulsing effects. The sample was contained in a cylindrical quartz cuvette of 20 mm in diameter. Together with extra-large optical windows in the vacuum shroud, this setup provides an accessible range of scattering angles from 20° to 155°, where an angle of 90° for the samples under investigation corresponds to a

scattering vector of approximately 2.1×10^{-3} Å^{-1}. In order to obtain reliable information on the sample temperature, the temperatures measured at the surface of the cuvette and at the heat exchanger were compared in a calibration run to temperatures measured right at the location of the scattering volume in a reference sample cell, resulting in an absolute accuracy of temperature measurement of $\Delta T \approx \pm 0.5$ K.

DATA ANALYSIS

In order to elucidate the properties of the different relaxations that appear in the binary mixtures, the following set of phenomenological relaxation time distributions was applied, from which either the frequency-dependent dielectric function

$$\hat{\varepsilon}(\omega) = \Delta\varepsilon \int_{-\infty}^{\infty} \frac{G(\ln \tau)}{1 + i\omega\tau} \mathrm{d} \ln \tau \quad (1)$$

or the time-dependent orientational correlation function probed in depolarized light scattering

$$\Phi_{\mathrm{depol}}(t) = \int_{-\infty}^{\infty} G(\ln \tau) \mathrm{e}^{-t/\tau} \mathrm{d} \ln \tau \quad (2)$$

were calculated.

For the primary α-relaxation a generalized gamma (GG) distribution is used, the properties of which were discussed previously[41,42]

$$G_{\mathrm{GG}}(\ln \tau) = N_{\mathrm{GG}}(\alpha,\beta) \mathrm{e}^{-(\beta/\alpha)(\tau/\tau_0)^{\alpha}} \left(\frac{\tau}{\tau_0}\right)^{\beta} \quad (3)$$

with $N_{\mathrm{GG}}(\alpha,\beta) = (\beta/\alpha)^{(\beta/\alpha)}\alpha/\Gamma(\beta/\alpha)$ being the normalization factor. This particular distribution allows, e.g., in contrast to Havriliak−Negami (HN) or Cole−Cole (CC) expressions, which are often applied to describe broad dielectric relaxation spectra, to calculate average relaxation times for all values of the shape parameters α and β[41]

$$\langle \tau \rangle = \tau_0 \left(\frac{\alpha}{\beta}\right)^{1/\alpha} \frac{\Gamma\left(\frac{\beta+1}{\alpha}\right)}{\Gamma\left(\frac{\beta}{\alpha}\right)} \quad (4)$$

with $\Gamma(x)$ denoting the regular gamma function. Of course this holds equally true for frequency- and time-domain data so that results of, e.g., dielectric and photon correlation spectroscopy will be compared based on the same phenomenological approach.

We note here that eq 2 also allows to disentangle the extra broadening of the spectra observed in binary mixtures in a particularly easy manner by simply replacing the exponential function in eq 2 by the correlation function $\Phi_{\alpha}^{\mathrm{neat}}(t)$ observed in the neat bulk substance. This procedure only requires that the experimental method to which it is applied selectively probes one of the components in the mixture. Then, the correlation function of this component in the mixture can be described by

$$\Phi(t) = \int G_{\mathrm{GG}}(\ln \tau) \Phi_{\alpha}^{\mathrm{neat}}(t/\tau) \mathrm{d} \ln \tau \quad (5)$$

Thus, if the relaxation function of, say, M-THF were the same in the mixture as in the neat system, $G_{\mathrm{GG}}(\ln \tau)$in eq 5 would become a δ-function if eq 5 were applied to describe $\Phi(t)$ in the mixture. In that case the parameter α of eq 3 would yield very large values in a fit (formally $\alpha \rightarrow \infty$). Note that for the α-relaxation of the neat components the time−temperature superposition principle is usually fulfilled to reasonable approximation so that $\Phi_{\alpha}^{\mathrm{neat}}(t/\tau)$ represents a well-defined average shape of the respective relaxation function.

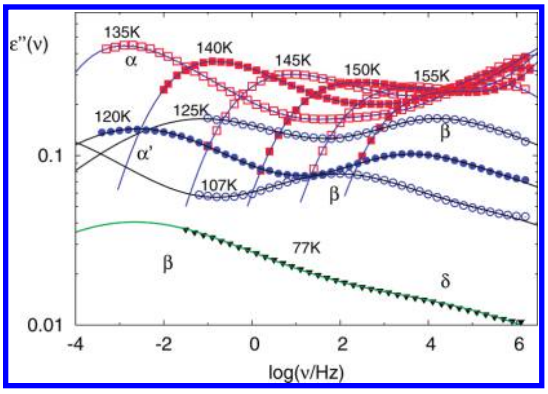

Figure 1. Dielectric loss of 50% M-THF in tristyrene. Beyond the main α-relaxation, three more processes can be identified, as indicated. Solid lines represent fits according to eq 3 and eq 6.

In dielectric spectroscopy, several processes faster than the slow α-relaxation are observed in the binary systems under study. For all of these relaxations, we used the following distribution of relaxation times, which is particularly suitable to model secondary processes in glass-forming systems[41]

$$G_{\beta}(\ln \tau) = \frac{N_{\beta}(a,b)}{b(\tau/\tau_{\mathrm{m}})^{a} + (\tau/\tau_{\mathrm{m}})^{-ab}} \quad (6)$$

with $N_{\beta}(a,b) = a(1+b)/\pi b^{b/(1+b)} \sin(\pi b/(1+b))$ being the normalization factor. The resulting dielectric function bears certain resemblance with the HN expression, as, e.g., it leads to power laws $\varepsilon'' \propto \omega^{a}$ and $\propto \omega^{-ab}$ $(0 < a, b \leq 1)$ on the respective sides of the dielectric loss peak. Apart from that, eq 6 has the convenient property that when the temperature dependence of the shape parameters is chosen as $a \propto T$ and b = const, eq 6 simply reflects an underlying temperature-independent distribution of activation energies,[41] which can be considered as the simplest type of thermally activated dynamics in a disordered system. As it was shown earlier, such a simple picture is found to hold for the β-relaxation in a large number of glass-forming liquids, in particular when in the framework of the generalized Eyring approach of activated processes[43] an additional distribution of activation entropies is considered together with the Meyer−Neldel rule (cf. ref 44 and references therein). Such a simple description of the evolution of the line shape is particularly convenient in case several overlapping relaxation processes have to be described, as it allows to model the temperature evolution of the spectral shape of secondary relaxations by globally adjusting only a few parameters. Note that, by contrast, the HN and CC expressions are not compatible with such a simple physical picture.[45]

An example of the application of eqs 3 and 6 is demonstrated in Figure 1 on the dielectric loss data of 50% M-THF in tristyrene. Further details will be discussed in section Dielectric Spectroscopy.

RESULTS AND DISCUSSION

In the following, we investigate the relaxation behavior of M-THF in tristyrene mixtures in the full concentration range

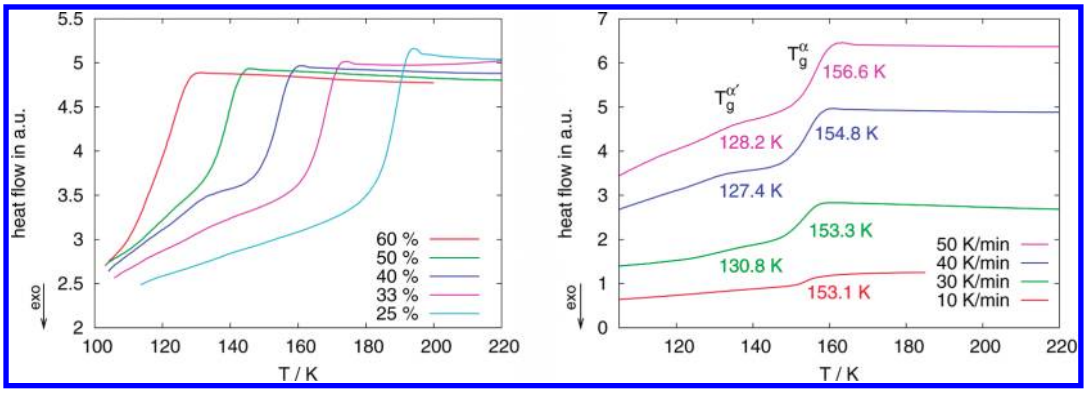

Figure 2. Temperature-dependent heat flow from DSC scans of M-THF in tristyrene mixtures at various concentrations of M-THF (given in wt %), obtained with a heating rate of 40 K/min (left). For comparison DSC scans for 40% M-THF in tristyrene at different heating rates are displayed (right).

from about 5 up to 70 wt % M-THF and compare it to the relaxation of the respective neat components. While differential scanning calorimetry contains information on all constituents of the sample, dielectric spectroscopy and depolarized light scattering enable us to selectively probe the dynamics of the small and the large molecules, respectively. NMR, on the other hand, is able to reveal details of the motional mechanisms involved and helps in identifying the nature of the observed secondary processes.

Differential Scanning Calorimetry. Although on a macroscopic scale M-THF and tristyrene form perfectly homogeneous and optically transparent mixtures at all temperatures and concentrations discussed in the present study, one of the most striking features is that two glass transition temperatures can be distinguished in DSC experiments. Similar to results reported previously,[16] a second glass transition step becomes discernible in the heat flow traces as the heating and cooling rate is increased, cf. Figure 2 (right). This second glass transition shows up most prominently in an intermediate concentration range, as can be seen in Figure 2 (left). Whereas for M-THF concentrations of 60% and above both glass transitions are too close to be separated, the second T_g step gets rather weak and can hardly be determined for concentrations of M-THF below 20%.

Traditionally, the existence of only one T_g in a binary glassy system was believed to be a criterion for miscibility of its components.[1] Recently, however, the existence of two glass transition steps in well-miscible binary systems was reported,[8,10,12,13,46] and also from a theoretical point of view two T_gs are expected for dynamically strongly asymmetric mixtures.[47]

In order to check whether any sign of macroscopic demixing occurs in our system, in particular upon cooling, we note first that the low-temperature glass transition step gets stronger with higher cooling rates. By contrast, if some kind of slowly ongoing phase separation occurred upon cooling, one would expect a bigger low-temperature step for lower cooling rates, contrary to observation. We also mention that the mixtures with a strong second glass transition were explicitly checked for long-time stability in an optical cryostat at temperatures slightly above the upper glass transition, where the overall dynamics is still fast enough to allow for macroscopic phase separation if it were to occur. However, no sign of turbidity or phase separation was observed.

Dielectric Spectroscopy. In contrast to calorimetric measurements, where both molecular components of the mixture appear with comparable strength, the dielectric experiments for

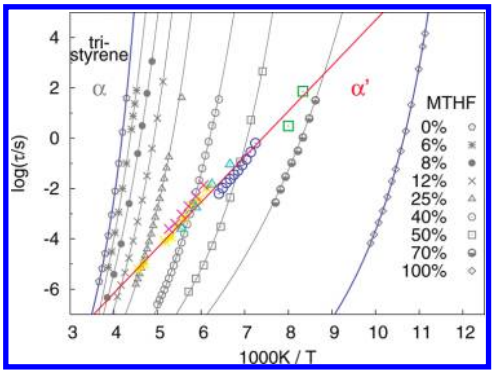

Figure 3. Main relaxation times of all the studied mixtures with M-THF (small symbols). Large symbols represent the α′-relaxation, which is also identified in calorimetry. The solid lines represent VFT functions in the case of the α-process. For the α′-relaxation an Arrhenius law is shown as guide to the eye.

the present mixtures under study almost exclusively reflect the reorientational motion of the smaller component, as the dielectric relaxation strength of M-THF, corrected for a Curie-type temperature dependence, is $T\Delta\varepsilon/100\ \mathrm{K} \approx 17.7$ compared to a value of 0.8 for tristyrene.

Figure 1 shows as an example data of the dielectric loss together with the fit results for a mixture of 50% M-THF in tristyrene. In Figure 3 the corresponding average α-relaxation times are shown for the mixtures together with τ_α for the corresponding neat systems and corresponding fits with a Vogel−Fulcher−Tammann equation.[48−50] Apart from the α-relaxation, altogether three faster processes can be identified in the dielectric spectra, e.g., in Figure 1. The time constants for the slowest of these additional relaxations, named α′, are also depicted in Figure 3 and are found to separate from the main relaxation process only at temperatures close to and below the upper glass transition. This process follows an Arrhenius-type temperature dependence in the frequency and temperature window where it is discernible and thus was analyzed in terms of eq 6 with a symmetric ($b = 1$) relaxation function. In particular at low concentrations of M-THF, where this process can be followed over a broad temperature range, the Arrhenius behavior becomes evident with an activation enthalpy of $\Delta H_a/k_B \approx 4200$ K, which is significantly lower than typical effective activation energies of the α-relaxation around T_g. This indicates that the dynamics of remaining mobile small molecules is strongly

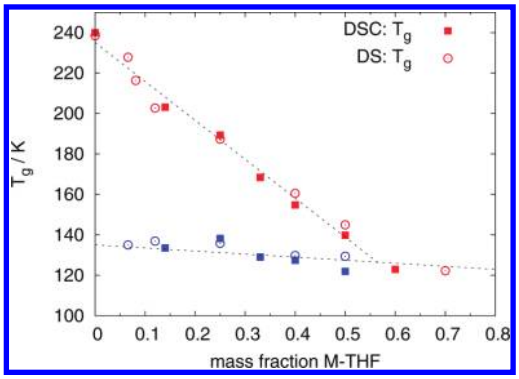

Figure 4. Glass transition temperatures obtained by DSC and dielectric spectroscopy of all the M-THF/tristyrene mixtures investigated. T_g from the dielectric loss spectra was obtained by using the relation eq 7.

influenced by the confining environment of that part of the mixture that already behaves nonergodic.

In order to compare the results from DSC and dielectric spectroscopy, we calculated a calorimetric time constant τ_{cal} for each of the calorimetric glass transition steps by using an expression given in ref 51

$$\tau_{cal} \approx \frac{k_B T_g^2}{\Delta H_{eff} Q_c} \quad (7)$$

where ΔH_{eff} is the effective average activation energy at T_g, which is estimated from the dielectric data, k_B is the Boltzmann factor, and Q_c is the cooling/heating rate applied in the calorimetric measurement. Then we extracted the temperature $T(\tau_{cal})$ at this particular relaxation time from the time constants of the α-relaxation (upper T_g) and the α′-relaxation (lower T_g) and thus arrived at T_gs from dielectric spectroscopy for each mixture. The results are presented in Figure 4. It becomes evident that the second glass transition step corresponds to a discernible relaxation peak in the dielectric data. Thus, as secondary relaxations are usually not active in calorimetric measurements, this particular process shall be termed α′ in the following. We note that for M-THF concentrations of 0.6 and above both processes and consequently both glass transition steps have merged completely, so that only one T_g remains visible in this particular concentration range, cf. Figures 2 and 4.

In order to further clarify the interplay between different relaxations, it is worthwhile to take a look at the respective relaxation strength of each process. Of course, this requires that the trivial temperature and concentration dependence of the relaxation strength can sufficiently be singled out. To check this, the overall relaxation strength was corrected for a Curie law and $T\Delta\varepsilon$ was plotted for all temperatures above T_g and all concentrations in Figure 5. In order to include all relevant relaxations in the overall $\Delta\varepsilon(T)$, the contribution of induced polarization ε_∞ was estimated from $\varepsilon'(\omega)$ at the lowest temperatures and assumed to be temperature independent to first approximation. Then, the static permittivity ε_s was extracted from the low-frequency limit of $\varepsilon'(\omega)$ and $T(\varepsilon_s(T) - \varepsilon_\infty)$ was plotted. Note that the values of $T\Delta\varepsilon(T)$ coincide on a single point for each concentration, indicating that the Curie law is fulfilled in very good approximation. Moreover, the overall relaxation strength evolves as a linear function of M-THF concentration as expected in the simplest case. Only the relaxation strength of neat M-THF does not fit into this picture and is about a factor of 5/4 larger than expected from an extrapolation of the relaxation strength

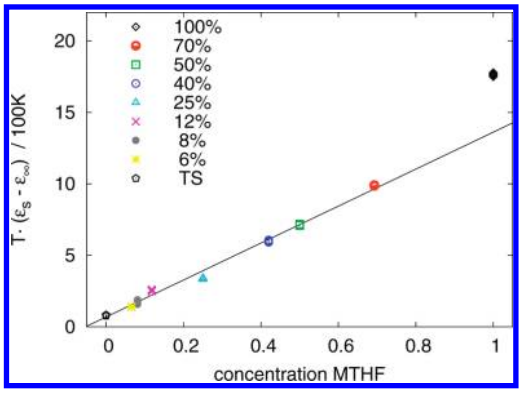

Figure 5. Overall dielectric relaxation strength of the M-THF/tristyrene mixtures extracted from the static dielectric constant taken on the low-frequency side of the α-relaxation and corrected for a Curie temperature dependence. For each concentration data of all available temperatures are shown. For a given concentration the points fall on top of each other.

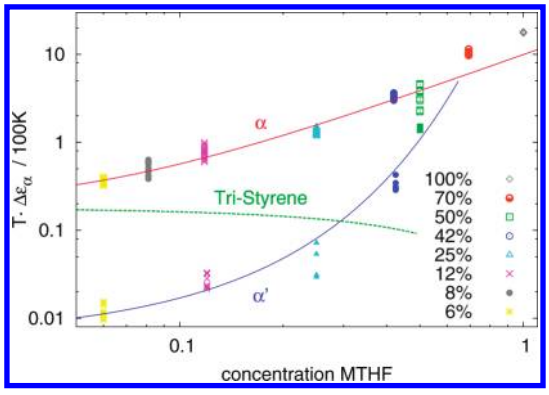

Figure 6. Dielectric relaxation strength of the α- and α′-relaxations for the investigated M-THF/tristyrene mixtures. For each concentration, all available data are shown, again corrected for a Curie-type temperature dependence. Solid lines are guides to the eye. Dashed line represents the expected contribution of the styrene molecules to the relaxation strength.

from lower concentrations. Most probably, this is due to nonvanishing Kirkwood correlations in neat M-THF, which are at least to some extent destroyed in the mixture.

Now, one can compare the relaxation strength of α- and α′-relaxations, which are corrected for the trivial temperature dependence. Thus, $T\Delta\varepsilon_\alpha$ is depicted in Figure 6 and it is seen that each process exhibits a temperature dependence of the relaxation strength beyond the Curie law, as the points for one concentration no longer coincide. For the α-relaxation, this is due to the temperature dependence of the strong β-process, which is found to increase significantly above T_g, most likely because the small angle of dipolar reorientation involved in the β-relaxation increases with temperature as it does in neat glass-forming systems.[52] The α′-relaxation for the tristyrene mixtures at lower concentrations of M-THF, where the separation of both processes is maximal, becomes so small that a clear temperature dependence of its relaxation strength is difficult to analyze.[83] Whereas $\Delta\varepsilon$ of the α-process varies more or less linearly with concentration, α′ decreases more strongly upon lowering the concentration, from about $0.5\Delta\varepsilon_\alpha$ at $c_{MTHF} = 0.5$ to about $0.03\Delta\varepsilon_\alpha$ in the low-concentration regime. However, when the

dx.doi.org/10.1021/jp110506z |J. Phys. Chem. B 2011, 115, 1623–1637

$\Delta\varepsilon$ values are compared with the expected contribution of tristyrene relaxation (dashed line in Figure 6), it becomes obvious that the small molecule M-THF necessarily takes part in both relaxation processes. In particular, the strength of the slowest α-process, which would naturally be assigned to the dynamics of the larger molecules in the mixture, is always significantly larger than the relaxation expected to arise from the tristyrene component. Thus, it becomes evident that the two time scales and T_gs in the mixture cannot be assigned to one component each, as it is frequently expected in the recent literature on binary systems with large dynamic asymmetry.[3] Rather, it seems that for the small component two dynamical species can be distinguished similar to findings for molecules confined in porous matrices, where different mobilities exist depending on the distance of a molecule from the confining wall.[53−55] The present finding is also in accord with previous findings reported by NMR spectroscopy, where the small molecules in binary mixtures showed characteristic two-phase spectra, indicating the presence of fast and slow small molecules in the mixture, even at temperatures close to and below the upper glass transition.[2,4]

Apart from the fact that the relaxation of M-THF in the mixture appears to be bimodal, the processes α and α′ are themselves broadened as compared to the main relaxation in neat M-THF: whereas eq 3 describes the α-peak of neat M-THF with parameters $\alpha = 10$ and $\beta \approx 0.8$,[39] similar to what is found in other glass-forming systems,[41] the α-relaxation in the present mixtures is significantly broadened. It is characterized by shape parameters of $\alpha = 1$ and $\beta \approx 0.3$ for low concentrations, which reduce to values of $\alpha = 0.5$ and $\beta = 0.1$ at intermediate concentrations, indicating an increased broadening and thus stronger concentration fluctuations at concentrations around $c_{MTHF} \approx 0.5$. The α′-relaxation, which follows an Arrhenius temperature dependence and thus is analyzed in terms of eq 6, can be described by a symmetric peak ($b = 1$) with a increasing from $a \approx 0.2$ in the 50% mixture to $a \approx 0.5$ at low concentrations, again indicating a stronger influence of concentration fluctuations in the intermediate concentration regime.

Concerning the temperature dependence of the line shape of α- and α′-relaxations, it is difficult to say whether systematic deviations from time−temperature superposition occur in the data, as the overlap of α-, α′-, and β-relaxations leads to significant scatter in the line-shape parameters. Thus, within rather large error bars of $\Delta\beta,\Delta b \approx \pm 0.1$, the data are consistent with $a \propto T$ for α′ and β = const for the α-relaxation. Hence, time−temperature superposition seems to hold for the α-process but not for α′, which rather shows a broadening typical of an Arrhenius temperature dependence upon cooling.

A common feature of all observed secondary relaxations is the Arrhenius-type temperature dependence, as can be seen in Figure 7, as well as the broadening of the process at lower temperatures (not shown) which is typical for secondary relaxations in glass formers[56] and to first approximation reflects the fact that a distribution of relaxation times actually corresponds to a distribution of activation energies. As there is a strong overlap of the secondary relaxations that appear in the mixture, an independent fit of the line-shape parameters of the β- and δ-relaxations was not attempted. Instead, the processes were assumed to be symmetric and for each process the underlying distribution of activation energies was assumed to be temperature independent, so that $a \propto T$ in eq 6 is a good approximation. In a global fit procedure including all concentrations and

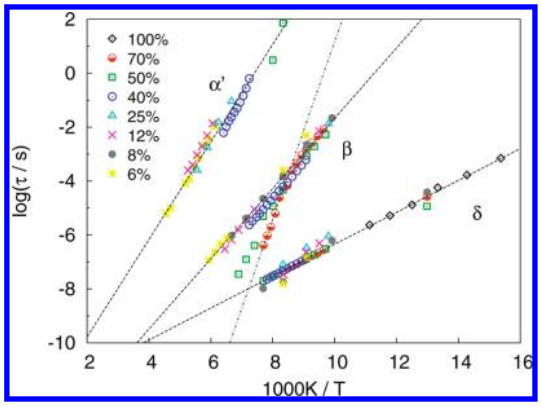

Figure 7. Relaxation times for the secondary β- and δ-relaxations in all the studied mixtures of M-THF and tristyrene. For comparison, the α′-relaxation is also shown. Dashed lines represent Arrhenius laws.

temperatures, it turned out that the proportionality factor for the δ-process could be chosen concentration independently so that $a_\delta = 0.0018T$ whereas for the β-relaxation a slight concentration dependence was introduced so that $a_\beta(c) = (0.001c + 0.002)T$, with c being the mass fraction of M-THF. In that manner, stable fits were achieved despite the strong overlap of several processes. An example of data and fits is shown in Figure 1 for a concentration of 50% M-THF. At other concentrations the fit results are of similar quality.

Figure 7 shows the time constants of the β-process, which obviously hardly depend on concentration with an activation energy of $\Delta H_a/k_B \approx 3000$ K. Similar to the findings in ref 37, the time constants of the β-relaxation follow this Arrhenius behavior only in the glass and up to the upper T_g of the mixture. Around the glass transition the relaxation times cross over to a much stronger temperature dependence, as can be seen for the data of 70% in Figure 7 indicated by the dash-dotted line with an activation energy of $\Delta H_a/k_B \approx 7600$ K. An onset of that behavior is also recognized in the 50% system, whereas for all other concentrations the β-process is only accessible below T_g.

For the fastest of the observed processes, the δ-relaxation, again hardly any concentration dependence is observed and the activation energy is found to be around $\Delta H_a/k_B \approx 1360$ K. In Figure 7 the fastest secondary process of neat M-THF is also included (100%, black diamonds) based on the data published in ref 39. We mention that the same relation $a_\delta = 0.0018T$ is used to describe the line shape of the δ-process in neat M-THF as in the mixtures. From the data in Figure 7 it becomes obvious that it would be of advantage to extend the measurements of the δ-process in the mixtures down to lower temperatures, as it was done for neat M-THF. However, the data of ref 39 were acquired in a liquid He cryostat, whereas the nitrogen gas cooling system available for the present experiments was limited to about 100 K toward low temperatures. Still, we were able to obtain one low-temperature measurement for a few concentrations by directly immersing the sample cell into liquid nitrogen, thus demonstrating that indeed the δ-process can be described by the same line-shape parameters and activation energies for all concentrations and is identical with the fastest process found in neat M-THF.

Concerning the β-relaxation in the mixtures, it turns out that it can be identified with the high-frequency wing observed in neat M-THF, similar to the observations previously made in mixtures of picoline and tristyrene.[37] This is demonstrated in Figure 8,

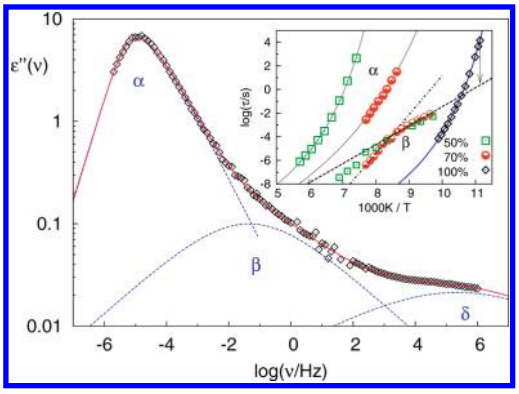

Figure 8. Dielectric loss of pure M-THF at $T = 89$ K (data adapted from ref 39). The solid line shows a fit with eqs 3 and 6, where the HF-wing contribution is described by eq 6 with parameters extrapolated from the β-relaxation identified in the mixtures. Inset: Relaxation times for α- and β-process at high concentrations of M-THF and the α-relaxation times of neat M-THF. The arrow indicates the time constant used to fit the HF-wing contribution in the main figure.

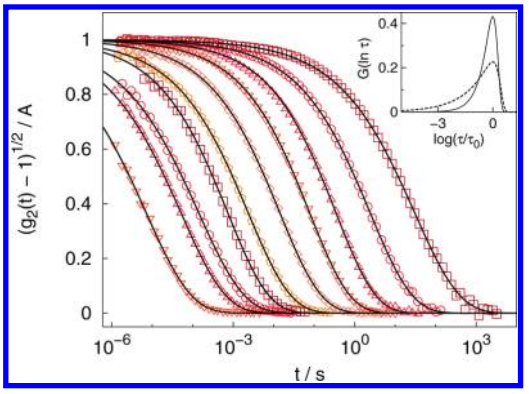

Figure 9. Correlation functions obtained by depolarized dynamic light scattering (vh geometry) in a mixture of 30% M-THF in tristyrene. Solid lines represent fits with eq 3 integrated in the time domain. Temperatures from right to left: 167, 170, 173.3, 176.3, 179.5, 182.6, 185.8, 188.8, 191.7, and 198 K. In order to demonstrate the influence of concentration fluctuations, the inset shows a distribution of $\Phi^{neat}(t)$ for the light scattering data at 170 K (solid line) compared to the corresponding distribution for the dielectric data at about the same temperature (dashed line), as suggested by eq 5.

where the time constant of the β-relaxation of neat M-THF at 89 K is extrapolated from the temperature evolution of τ_β in the mixtures below T_g according to the Arrhenius law, as indicated by the arrow in the inset of Figure 8. Moreover, the line-shape parameter in eq 6 is set to $a_\beta = 0.003T$ consistent with the concentration dependence $a_\beta(c)$ obtained in the fits of the β-relaxation in the mixtures. Thus, the high-frequency wing smoothly emerges out of the temperature evolution of the line shape of the β-process observed as a separate peak at low and intermediate M-THF concentrations. We also mention that 89 K is the lowest temperature, where the full α-peak is visible in the available frequency window of the data from ref 39. At that temperature the α-relaxation and the high-frequency wing-process are best separated, in order to provide a convenient consistency check for the above analysis.

Of course, the simple fact that the secondary relaxations can be assigned to relaxation processes observed in neat M-THF does not imply an understanding of their nature. Still, the similarity to previous findings[37,38] suggests that actually the high-frequency wing relaxation in neat M-THF and the corresponding β-peak in the mixtures have to be identified with the Johari−Goldstein β-relaxation typical for many glass-forming systems.[56−58] Further light will be shed on this issue when the results of NMR spectroscopy on a comparable system of THF in tristyrene are discussed in the Dielectric Spectroscopy Revisited section. But before that we turn to dynamic light scattering, which is complementary in the sense that it allows us, together with the dielectric data, to directly compare the α-relaxation of both components in the blend.

Dynamic Light Scattering. In order to access the dynamics of the larger molecules in the mixture, we performed depolarized dynamic light scattering (DDLS). In our particular system, M-THF is selectively probed by dielectric spectroscopy whereas tristyrene is selectively probed as the optically anisotropic component by DDLS. We note here that we were not able to record correlation functions in vh geometry of neat M-THF at temperatures slightly above T_g due to the low depolarization of M-THF. Thus, molecular reorientation of the optically anisotropic component tristyrene is exclusively probed in our experiment. We obtain the normalized field autocorrelation function of the scattered light in the ergodic regime above the upper T_g via the Gaussian approximation[59]

$$g_1(t) = \left(\frac{g_2(t) - 1}{f}\right)^{1/2} \tag{8}$$

from the normalized intensity autocorrelation function $g_2(t) = \langle I(\tau)I(\tau + t)\rangle/\langle I^2(\tau)\rangle$, with a coherence factor of $f = 0.33$ due to the properties of the optical fiber in use.[84]

The field autocorrelation functions of a mixture of 30% M-THF in tristyrene are shown in Figure 9. For all temperatures, broad correlation functions were found, which were analyzed by integrating eq 3 in the time domain, in order to be fully consistent with the analysis of the dielectric data. As for the α-relaxation in the dielectric data, the line shape was characterized by one fixed α-parameter for each concentration, while β was allowed to be temperature dependent. Besides the mixture with 30% M-THF in tristyrene, a mixture with 50% M-THF and pure tristyrene was measured. It turned out to be a good choice to fix $\alpha = 0.7$ for the DLS measurements at all concentrations including neat tristyrene. Still, the relaxation becomes broader with increasing M-THF content as β decreases from 0.58 ± 0.04 in pure tristyrene to 0.40 ± 0.03 and 0.23 ± 0.02 in the 30% and 50% mixtures, respectively. Within the indicated error bars, the time−temperature superposition principle was found to be fulfilled for the tristyrene relaxation in the neat system as well as in the mixtures.

While in the absence of interaction-induced effects DDLS probes the reorientation of optically anisotropic molecules, dynamic light scattering in polarized (vv) geometry is in addition sensitive to concentration fluctuations in the case of a binary mixture, due to the isotropic part of the polarizability tensor. For the mixture of 30% M-THF in tristyrene, several vv-correlation functions for a fixed temperature of 192 K at different scattering angles θ are shown in Figure 10. The fast angular-independent relaxation corresponds to the depolarized part contained in the polarized scattering[59] and thus to reorientational dynamics. The slow relaxation is identified with long-range concentration fluctuations, which relax by collective diffusion, so that the average relaxation times obey a diffusive wave vector dependence

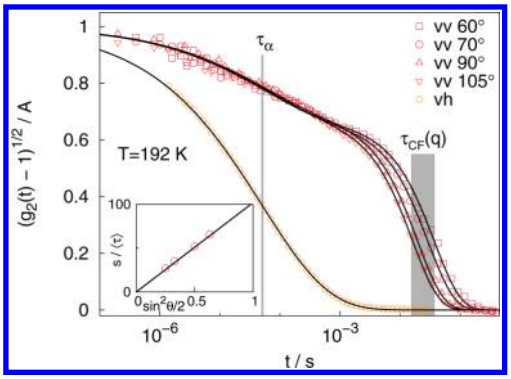

Figure 10. Correlation functions obtained by polarized dynamic light scattering in a mixture of 30% M-THF in tristyrene at T = 192 K at different scattering angles. The contribution due to concentration fluctuations and the one due to molecular reorientation are clearly discernible. The fits were done by combining eq 3 with a single-exponential relaxation as described in the text. For comparison the vh correlation function at the same temperature is shown. The vertical bars indicate the scattering angle dependence of the correlation time of the different types of processes. The inset shows $1/\tau_{vv}$ as a function of q^2.

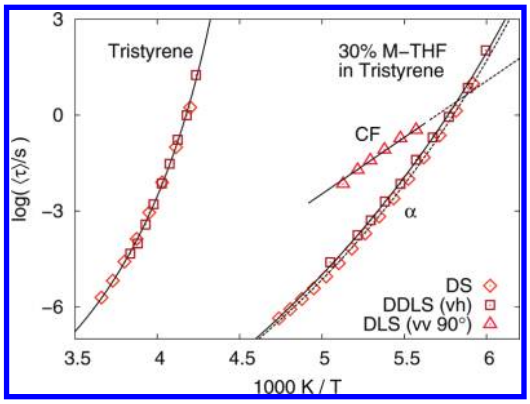

Figure 11. Average relaxation times of depolarized dynamic light scattering (squares) compared to the α-relaxation times obtained in dielectric spectroscopy (diamonds) and the relaxation times of concentration fluctuations (CF) from polarized light scattering at an angle of 90°.

$\langle\tau\rangle^{-1} \propto \sin^2\theta \propto q^2$, as demonstrated in the inset of Figure 10 for the chosen temperature. Here, $q = (4\pi n)/\lambda \sin\theta/2$ is the absolute value of the scattering vector, with n and λ being the index of refraction of the medium and the wavelength, respectively. The fits of the vv data are done by combining the vh fit result (the corresponding measurement is also shown in Figure 10) with a single-exponential decay. Due to the different shape of the two relaxations ($\beta_\alpha \approx 0.4$ and $\beta_{CF} \approx 1$), both processes can be distinguished even very close to the matching point of both relaxations, as the independent information of the vh data is included in the analysis.

In Figure 11, the DDLS average relaxation times for the α-process in pure tristyrene and in 30% M-THF in tristyrene are compared to results obtained in dielectric spectroscopy (DS). The DS and DDLS data for neat tristyrene perfectly lie on top of each other. As dielectric and photon correlation spectroscopy are known to probe orientational correlation functions of the first and second rank Legendre polynomial, respectively,[59] this result indicates that the geometry of the underlying molecular reorientation is such that the relaxation times are, to first approximation, insensitive to this difference, as would, e.g., be the case if one assumes a randomized uniform distribution of jump angles.[59]

For the mixture the relaxation times coincide within the experimental error bars corresponding approximately to the symbol size. We note that in the mixture both experimental techniques probe different species of molecules. Hence, this result indicates that to first approximation there is no dynamic decoupling between the α-relaxation of M-THF and tristyrene in the mixtures. The time constants for correlation functions of l = 1 and l = 2 Legendre polynomials $P_l(\cos\theta(t))$ differ at most by $\tau^{l=1} = 3\tau^{l=2}$ in the case that preferentially small jump angles are involved in the reorientational process under consideration.[59,60] Thus, our data indicate that the α-relaxation of M-THF can at maximum be by a factor of 3 faster than the α-relaxation of the styrene molecules. Thus, the former does not significantly decouple from the matrix relaxation in the system.

Coming back to Figure 11, we note that the temperature dependence of the α-relaxation times are well described by a Vogel−Fulcher function. In contrast, the relaxation times for concentration fluctuations τ_{CF} obtained by vv-DLS, which are also given in Figure 11, follow an Arrhenius law. It is particularly striking that even when the α-relaxation times approach the characteristic times of the concentration fluctuations, the latter seem to be unaffected and maintain thermally activated behavior. In a recent publication,[16] we have shown by photon correlation spectroscopy with coherent X-rays (XPCS) that for a similar binary system the concentration fluctuations relax close to and below the intersection point with the same Arrhenius behavior as for higher temperatures. If this had to be considered as an equilibrium property of the system, it would imply that CFs can no longer be considered stationary close to T_g. However, at temperatures below the intersection point the system showed clear signs of ergodicity-breaking in the XPCS experiments, so that the situation is difficult to judge.[16] Of course, this adds to the difficulties in a conventional DLS experiment, where CFs and reorientational contributions are anyway hard to disentangle around the intersection point. In Figure 11 CFs are thus only shown in the range where both components could be unambiguously disentangled in the relaxation functions of vv scattering.

In binary mixtures, the concentration fluctuations are expected to lead to a distribution of local T_gs and thus of local relaxation times that in turn lead to overall broader relaxation functions compared to the neat components. In order to judge the effect of concentration fluctuations on the width of the α-relaxation of both components, we also analyzed the α relaxations of M-THF and tristyrene in the mixtures in terms of a distribution of relaxation functions, the shape of which is determined by the relaxation of the pure components as suggested by eq 5.

We applied this approach to the tristyrene and M-THF relaxations as obtained by DS and DDLS by inserting $\Phi_\alpha^{MTHF}(t/\tau)$ as obtained in the respective neat substance into eq 5 or the equivalent frequency domain expression. We particularly checked the 30% and 50% mixtures, as these showed the largest broadening. First of all, the resulting fit curves are virtually indistinguishable from the direct fits of eq 3 to the data, as they are shown in Figure 9. As it is demonstrated for a temperature around T_g in the inset of Figure 9, it turns out that the distribution of $\Phi_\alpha^{MTHF}(t/\tau)$ required to describe the M-THF relaxation in the mixture is significantly broader than the distribution of $\Phi_\alpha^{tristyrene}(t/\tau)$ necessary to describe the relaxation of tristyrene molecules in the DDLS spectra for the same system. Quantitatively, at a temperature of $T \approx 170$ K in a

mixture with 30% M-THF, $G_{GG}(\ln \tau)$ in eq 5 is characterized by $\beta \approx 0.33$ for M-THF and $\beta = 0.84$ for tristyrene, both with $\alpha = 2.0$. In terms of the distributions' full width at half-maximum, a width of 1.54 decades compares to a width of 0.87 on a log τ scale. Similarly, in the 50% mixture a width of 3.7 decades for the M-THF distribution compares to a width of 2.3 decades for the one of tristyrene. As the inherent difference of the spectral shape caused by using different experimental methods is already contained in each $\Phi_\alpha^{neat}(t/\tau)$, we can draw two conclusions: first, the relaxation functions in the mixtures are broadened as compared to the respective neat systems, and second this broadening effect shows up in an asymmetric way, as the small molecules seem to be more affected by the concentration fluctuations than the large ones. We note that this finding is in accord with previous observations by NMR spectroscopy, where the typical two-phase spectra were only identified for the smaller molecular component.[2]

To understand the effects of concentration fluctuations on the relaxation spectra in binary mixtures, it is frequently noted that the cooperative volume plays a crucial role in that it determines the volume over which a concentration fluctuation has to occur in order to have an effect on the α-relaxation.[19] From the simple concentration fluctuation models that consider a temperature-dependent cooperative volume, an equal effect on both components is expected, when the average relaxation times of each component are about equal.[17] Only if each molecular species averages the local concentration over a different cooperative volume that is not directly linked to the temperature evolution of the time constants, as suggested in ref 20, a different respective broadening of the relaxation of both components with at the same time identical average relaxation times can be rationalized. In that case, our findings would suggest that the smaller molecules are associated with a smaller cooperative volume so that local concentration fluctuations become more effective for the broadening of the relaxations, as large fluctuations are more likely to occur in small reference volumes.[18,61]

Dielectric Spectroscopy Revisited: Influence of the Methyl Group. To proceed one step further in particular in identifying the nature of the secondary β- and δ-relaxations, we replaced M-THF by THF (tetrahydrofuran) in some of the mixtures, first of all in order to clarify whether the basic phenomena are the same without the methyl group attached to the THF ring and thus to single out the influence of the methyl group on the main and secondary relaxations, and second, because deuterated THF-d_8 is readily available and opens up the possibility to further clarify the nature of the secondary relaxations by NMR spectroscopy, as will be discussed further in the next section.

We note first that bulk THF has a very strong tendency to crystallize when being supercooled and thus, to our knowledge, the glass transition temperature of neat THF is not known. Even the binary mixtures are not stable against crystallization for high concentrations of THF. Therefore, our experiments with mixtures containing THF were restricted to THF concentrations of ≤33% as these mixtures did not show crystallization. Figure 12 shows the average α-relaxation times of three mixtures from this stable concentration regime as compared to the relaxation times shown for the M-THF mixtures in Figure 3. One observes that the relaxation times are very similar. As the density and molecular weight of both THF and M-THF are comparable, a given concentration by weight implies about the same number of solvent molecules in a given sample volume of both types of

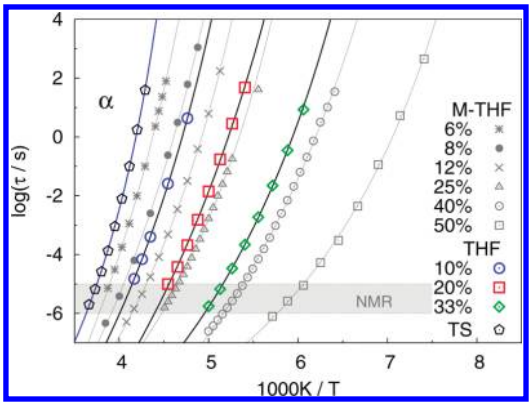

Figure 12. Average α-relaxation times of three mixtures of THF in tristyrene (large symbols) in comparison to the α-relaxation times of some M-THF mixtures. Small symbols and light solid lines are identical to those in Figure 3. For reference, the time window relevant for understanding the NMR spectra is marked by a horizontal bar.

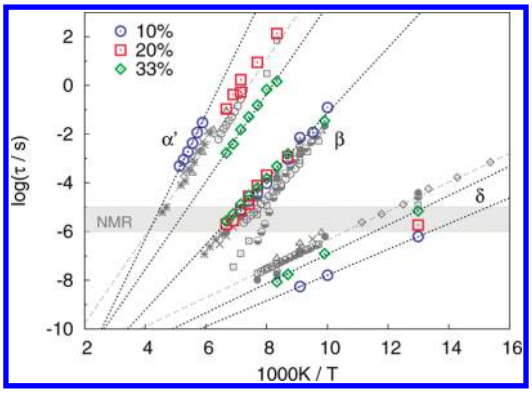

Figure 13. Relaxation times of the α′ and the secondary β- and δ-relaxations of the THF/tristyrene mixtures (large symbols). For comparison, the respective relaxation times are shown for the M-THF mixtures (small symbols); cf. also Figure 7.

mixtures. Thus, the respective concentrations can indeed be compared and the glass transitions and the α-relaxation dynamics are close to being identical in both types of mixtures. The same holds true for the line-shape parameters, where, e.g., $\alpha = 0.7$ and $\beta = 0.3$ describe the broadening of the α-relaxation of THF in the mixture with $c_{THF} = 0.2$.

Apart from the α-relaxation, all other relaxation processes that were previously identified in the M-THF mixtures can be equally identified in the mixtures with THF. As Figure 13 demonstrates, the time constants of the α′-relaxation are very similar compared to the ones found in the M-THF mixtures, thus demonstrating that the process responsible for the second glass transition is equally observed in the THF mixtures. As only difference should be mentioned that $\tau_{\alpha'}$ shows a slightly stronger concentration dependence in the THF mixtures than in the ones with M-THF, where in the small temperature interval in which the α′ relaxation is discernible, almost the same Arrhenius law is found independent of concentration.

The β-relaxation, on the other hand, does not show any sign of concentration dependence in the THF mixtures and is located at the same time scale with the same activation energy as for the systems containing M-THF. This emphasizes the local nature of the β-relaxation, which was identified as the excess wing in neat

dx.doi.org/10.1021/jp110506z |J. Phys. Chem. B 2011, 115, 1623–1637

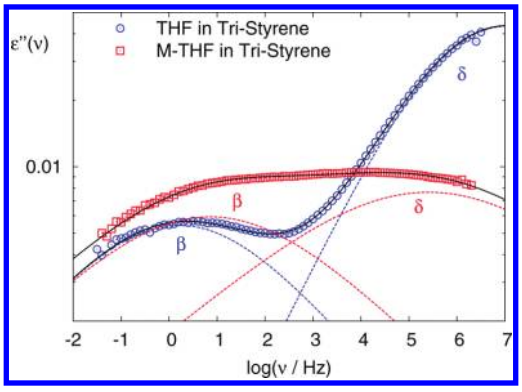

Figure 14. Secondary β- and δ-relaxations in two mixtures of comparable concentration of 8% THF and M-THF in tristyrene, both at $T = 100$ K. Solid lines are the fits with eq 6, and dashed lines represent the respective contribution of each process to the spectrum.

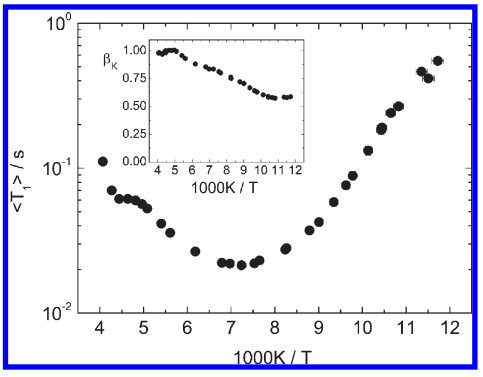

Figure 15. Average spin−lattice relaxation time of THF-d_8 as a function of the inverse temperature. The inset shows the stretching parameter β_K, which demonstrates that T_1 becomes nonexponential as the upper glass transition of the mixture is approached.

M-THF and seems to appear at the same time scale also in THF. Further below it will be discussed in the context of NMR spectra that the angle of reorientation involved in this process must be very small, thus showing the typical features of a Johari−Goldstein relaxation.

The δ-relaxation, on the other hand, is slightly faster in the THF mixtures and shows a certain concentration dependence, however, without a significant change in activation energy. Still, the time constants are very close to those found in the mixtures with M-THF, so that all in all the relaxation times behave very similar in both types of blends. In fact, the most significant difference is seen in the relaxation strength of the δ-process. As an example, Figure 14 shows the β- and δ-relaxations of mixtures of THF and M-THF in tristyrene, both at a temperature of $T = 100$ K and at a comparable concentration of 10% and 8%, respectively. Both processes are slightly more separated in the THF mixture, as is indicated by the time constants displayed in Figure 13, and the β-process displays a comparable relaxation strength in both systems. The δ-relaxation, by contrast, is by about a factor of 5 stronger in the THF system. At the same time the δ-relaxation is significantly more narrow, with a line-shape parameter of $a = 0.45$ as compared to $a = 0.18$ in the M-THF mixture at the same temperature. Of course, such findings are hard to understand unless one has at least some idea about the motional mechanisms behind the secondary relaxations that appear in the blend. Thus, we performed ^{2}H NMR experiments on a sample of 30% THF-d_8 in tristyrene, in particular to elucidate the nature of the secondary relaxations in the mixtures.

NMR Spectroscopy. The phenomenon exploited in ^{2}H NMR spectroscopy is the interaction of the deuteron electrical quadrupole moment with the electric field gradient (EFG) present at the site of the nucleus. The EFG is dominated by the charge distribution generated by the σ-bond between the deuterium and, in our case, a carbon atom (C−^{2}H bond). The tensor of the EFG is axially symmetric in good approximation, with the C−^{2}H bond representing the symmetry axis, and the NMR frequency in the rotating frame only depends on the angle θ between the bond direction and the external magnetic field:[40]

$$\nu(\theta) = \pm\frac{\delta}{2}[3\cos^2(\theta) - 1] \qquad (9)$$

where δ is the anisotropy parameter. Thus, the rotational motion of the C−^{2}H bond is directly monitored by a change in ν.

A sample with an isotropic distribution of angles θ (powder) and with C−^{2}H bonds undergoing a rotational motion with a correlation time τ that fulfills $\tau \gg 1/(2\pi\delta) \approx 10^{-6}$ s (slow motion limit) gives rise to a Pake spectrum.[40,62] If $\tau \ll 1/(2\pi\delta)$ holds (fast motion limit), then the spectrum loses its structure. If the motion is isotropic, or at least of cubic symmetry, one observes a narrow line. Around the time scale of the inverse anisotropy parameter, the spectrum reveals strong changes reflecting the geometry and time scale of molecular motion. Usually, these effects are most pronounced in a time window of $1/(2\pi\delta) \le \tau \le 1/\delta$.[63] For comparison with the dielectric data, this time window is marked in Figures 12 and 13.

To investigate the spin−lattice relaxation, we measured the buildup of the longitudinal magnetization after it was set to zero by a saturation sequence. The experimental data curves were fitted with a stretched exponential function $M(t) = M_\infty[1 - \exp(-(t/T_1)^{\beta_K})]$ and the average spin−lattice relaxation time was calculated as $\langle T_1 \rangle = T_1/\beta_K\Gamma(1/\beta_K)$, with Γ denoting the regular gamma function.[64] The spin−lattice relaxation time is proportional to the inverse of the spectral density of motion at the Larmor frequency ω_L,[65,66] hence it does not reveal any details about the motional mechanism. Nevertheless, at the temperature of the T_1-minimum one can determine a rotational correlation time $\tau \approx 1/\omega_L$.[65,66]

In Figure 15 the average spin−lattice relaxation times and the stretching exponent of the longitudinal magnetization recovery curves are displayed. One observes that $\langle T_1 \rangle$ shows a minimum at a temperature of about $T \approx 135$ K. As mentioned above, at this temperature the rotational correlation time is characterized by $\tau \simeq 1/\omega_L$, where $\omega_L = 2\pi 46.2$ MHz in our case. This leads to an estimate of a rotational correlation time on the order of 10^{-9} s at 135 K. When this result is compared with the dielectric relaxation times displayed in Figure 13, we can conclude that the relaxation process in question has to be identified as the δ-relaxation seen in the dielectric data.

The stretching exponent is $\beta_K < 1$ at temperatures lower than about 200 K and ≈1 at higher temperatures. Such a behavior is expected when, with lowering the temperature, the sample approaches its glass transition. In this case, τ_α becomes longer than the average spin−lattice relaxation time and molecular dynamics does not average over relaxation components originating from different sites in the amorphous material. Hence, one observes a distribution of spin−lattice relaxation times reflecting a distribution of rotational correlation times.

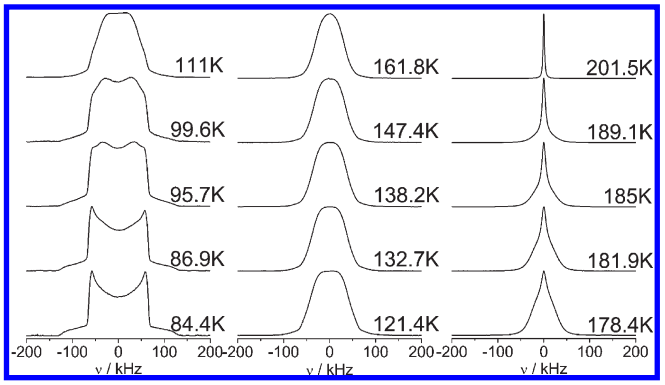

Figure 16. Temperature dependence of the solid-echo spectra normalized to their maximum.

We proceed by showing in Figure 16 the solid-echo spectra measured in a large temperature range. At the lowest temperature the spectrum resembles a Pake pattern,[40,62] and, with rising temperature, the spectral shape changes. From 121.4 until 161.8 K the shapes of the spectra are, to first approximation, identical. At 178.4 K a narrow line emerges in the central part of the spectra. The weight of this line increases with temperature so that at the highest temperature it is the only component of the spectrum.

First, we focus on the central column of Figure 16: the spectra from 121.4 until 161.8 K are virtually temperature independent. Therefore, one can conclude that they correspond to a process with a rotational correlation time which is out of the ^{2}H solid-echo time window. As the shape is not that of a Pake spectrum, we further conclude that the process must be in its fast motion limit $\tau \ll 1/(2\pi\delta) \approx 10^{-6}$ s. This, together with the results from dielectric spectroscopy and spin−lattice relaxation times, leads to the conclusion that the spectra in the central column of Figure 16 show the fingerprint of the δ-relaxation in its fast motion limit. As the spectra are broad, the motional process must be restricted reorientation; that is, the C−^{2}H bonds do not explore the entire unit sphere in their rotational motion. In contrast, for an isotropic rotational process in its fast motion limit, one expects a narrow line like, for example, the one measured at 201.5 K.

The δ-process that is in its fast motion limit at temperatures larger than 121 K will pass through the ^{2}H solid-echo time window at lower temperatures. That is exactly what is seen in the left column of Figure 16. At the lowest temperature of 84.4 K the spectrum resembles a Pake pattern, proving that the δ-relaxation almost exited the ^{2}H solid-echo time window reaching its slow motion limit $\tau \gg 1/(2\pi\delta) \approx 10^{-6}$ s. At temperatures between 86.9 and 111 K the spectra are temperature dependent, reflecting the passage of the restricted rotational process through the NMR time window. Although this passage might be expected to occur at slightly lower temperatures when judging from the dielectric time constants of Figure 13, one has to consider that a broad distribution of relaxation times passes through the NMR time window so that a significant part of this distribution represents relaxation slower than 10^{-5} s even at a temperature of, say, 100 K as can be seen, e.g., in the δ-spectrum of Figure 14. As no other relaxation is close to that time scale in this temperature window, clearly the δ-relaxation is responsible for the line-shape changes.

Note that the spectra are very different from what is typically seen for a Johari−Goldstein (JG) β-process.[52,67,68] In the latter case the spectra for a comparably short solid-echo interpulse delay of $t_p \approx 25$ μs are similar in shape to a Pake spectrum even though the corresponding rotational correlation times lie within the relevant time window. The reason is that the rotational motion corresponding to the JG β-process is so highly restricted that it has only a slight effect on such spectra.[52,67,68] For example, assuming that the C−^{2}H bonds only move on a cone, which is a model for restricted reorientation, one estimates that semicone angles of about 4° suffice to explain the experimental findings.[52,67,68] Thus, we conclude that for THF, although the rotational motion is restricted, the C−^{2}H bonds explore considerably larger angles than those involved in a JG β-process.

When looking for similar spectral shapes in the literature, one should mention a ^{2}H NMR study of a clathrate hydrate of THF-d_8[69] reporting comparable line shapes. The origin of the line shape was interpreted as being the puckering motion of the THF ring,[70] although this was challenged in a recent thorough paper[71] which proposed that the crystal geometry of the clathrate hydrate dictates the reorientation of the THF molecule as a whole unit. However, as in our case the sample is amorphous, we prefer to test the hypothesis that the spectral shape is due to some kind of puckering motion.

Rayón and Sordo, who performed ab initio calculations for THF, reported two possible configurations,[72] S1 and S2 in the terminology of their paper, in addition to the planar configuration S0. S1 is a global minimum in a conformational energy landscape and S2 a local minimum.[72] From the ab initio calculation, one expects that the S1 and S2 configurations are favored compared to the planar one, leading to a so-called pseudorotation of the THF ring.[72] However, the relatively large activation energy of the δ-process leads us to consider a model which also takes into account a transition between S1 and S2 through the planar S0 configuration.

If the geometry of the conformation is known, one can simulate the ^{2}H spectra corresponding to conformational jumps. Details concerning ^{2}H spectra simulations can be found, e.g., in refs 40, 73, and 74. We simulated the ^{2}H spectra corresponding to a S1−S0−S2 conformational jump using the distribution of rotational correlation times and its temperature dependence as obtained from dielectric spectra for the δ-process. It was assumed that a jump from the S1 to the S2 configuration and vice versa does not occur directly in the sense of a pseudorotation as discussed in ref 72 but rather by passing through the S0 configuration. From the S0 configuration any of the other two available configurations is obtained with equal probability (S1−S0−S2 model). Figure 17 shows the simulated spectra in the left column along with the measured ones in the central column. One sees that the simulated spectra do not reproduce the experimental ones. We conclude that the dynamical motion that leads to the experimental spectra cannot be the exact S1−S0−S2 scenario. As the THF molecule is in an amorphous mixture, one may expect that the puckering motion might be influenced by its environment and be different from the motion in a gas phase. Hence, we refine the motional model by allowing for geometrical distortions in the S1−S0−S2 scenario. This is implemented by randomly choosing the position of a C−^{2}H bond for a certain configuration (S1, S0, or S2) within a cone with an opening semiangle of ϕ and its axis the orientation of the bond in the original molecular configuration predicted by the ab initio calculations. The geometries of the so-obtained sites are randomly chosen for different C−^{2}H bonds but remain constant for a specific C−^{2}H bond during the whole simulation time.

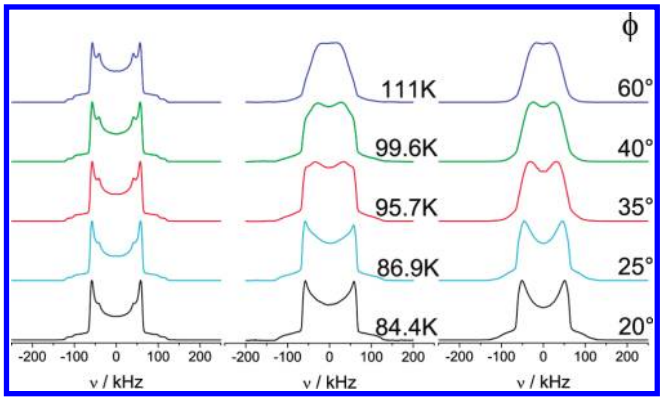

Figure 17. Experimental spectra measured between 84.4 and 111 K (central column); the simulated spectra corresponding to a S1−S0−S2 conformational jump scenario (left column); and the spectra corresponding to the distorted S1−S0−S2 scenario (right column), ϕ is the distortion angle. Again, all spectra were normalized to their maximum.

Figure Figure 17, right column, shows the spectra obtained by using the above-mentioned distorted S1−S0−S2 model. The best resemblance between simulations and measured spectra was obtained by allowing the semicone angle to increase with the temperature. Now the simulation reproduces the experimental data in a satisfactory manner, which supports the interpretation of the δ-process as an internal motion of the THF ring.

We refer once more to the spectra in the central column of Figure 16. From dielectric spectroscopy we know that $\tau_\beta \approx 1/(2\pi\delta) \approx 10^{-6}$ s in the temperature range 120−160 K (cf. Figure 13). So, it is clear that the effects of the β-relaxation on the NMR spectra are seen in this temperature range. As these effects are only subtle, the angular amplitude of the molecular motion associated with this process must be small, considerably smaller than the amplitude of the conformational jump process connected with the δ-relaxation and thus more typical of a JG β-process. Thus, although a further analysis becomes difficult due to the motional narrowing of the spectra by the δ-relaxation, the NMR spectra are so far consistent with identifying the β-process as the actual JG β-relaxation. In particular, the β-process cannot involve large angle jumps as they are, e.g., identified for the δ-relaxation in the NMR spectra.

Finally, we briefly discuss the spectra in the right column of Figure 16. One recognizes that their shape looks like a sum of a broad spectrum and a narrow one. The spectra were fitted by a sum of the experimental spectrum at 161.8 K and a Lorentz line with a weighting factor W. The fitted results are shown in Figure 18 and obviously the experimental data are reproduced very well, confirming that the spectra are so-called "two-phase" spectra.[2,15,75−78] It turns out that the spectra show the passage of the α-relaxation through the ^{2}H solid-echo time window: below 161.8 K and above 201.5 K this process is in its slow and its fast motion limit, respectively, as can be confirmed by comparing the dielectric α-relaxation times of the 33% mixture in Figure 12 with the relevant NMR time window. From the fact that the high-temperature spectrum is a narrow line, we conclude that the process involves isotropic reorientation and thus has to be identified as the α-relaxation. The spectrum at temperatures of about 180 K is a superposition of the spectrum in the slow motion limit and one corresponding to a fast motion; this is the signature of a very broad distribution of rotational correlation times. The distribution is so broad that both slow $\tau_\alpha \gg 1/(2\pi\delta)$

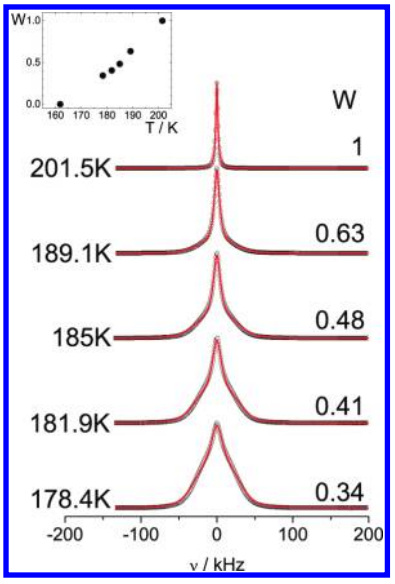

Figure 18. Results of a fit of the spectra shown in Figure 16, right column; circles, experimental data; line, fit. W is the relative weight of the Lorentz line. Inset: the temperature dependence of W.

and fast $\tau_\alpha \ll 1/(2\pi\delta)$ subensembles are present at a given temperature. Such spectra are usually not observed for bulk organic glass formers where the spectra transform continuously from a slow motion limit spectrum to a Lorentz line upon heating. It is argued that the width of the distribution of correlation times is too small to provide such "two-phase" spectra,[75] whereas they are frequently reported in dynamically asymmetric binary mixtures[2,15,75] or for glass-forming liquids in confinement.[15,76−78] In such systems they are considered as hallmarks of particularly pronounced dynamic heterogeneity, and indeed the parameters that describe the line shape of the dielectric α-relaxation of 20% THF in tristyrene indicate significant broadening consistent with the broadening observed in the M-THF mixtures at comparable concentrations, as discussed earlier in the Differential Scanning Calorimetry section. Note, however, that two-phase spectra do not necessarily indicate that the isotropic reorientation is bimodal. In the present case, the α- and α′-relaxations are only found to clearly separate rather close to T_g in a dynamic range where both processes have reached the slow-motion limit of NMR ($\tau \gg 10^{-6}$ s, cf. Figure 12). Although it may well be that the two-phase spectra are due to the existence of the α′-relaxation, the underlying distribution of relaxation times is very broad but still monomodal in the corresponding temperature range. In systems with even higher T_g contrast, such effects could be disentangled. This will be subject of future investigations.

SUMMARY AND CONCLUSIONS

In the present study, we investigated the component dynamics in mixtures of the glass former M-THF with tristyrene. Although both substances are macroscopically well miscible, it turns out that for M-THF concentrations below 60% two separate glass transitions can be detected in calorimetry. These glass transitions are equally well resolved in dielectric spectroscopy, which selectively probes the molecular reorientation of M-THF due to the large contrast in dipole moment. Thus, the small molecule in the mixture takes part in both T_g-associated relaxations.

Interestingly, the slowest dielectric relaxation, the α-process of M-THF in the mixture, shows a relaxation time, which is identical with the time scale of the reorientation of tristyrene molecules detected by photon correlation spectroscopy. Still, the faster dielectric process α′ indicates that the motion of a significant amount of M-THF molecules is decoupled from the matrix relaxation, as the latter freezes out at the upper T_g of the mixture, while the former retain their mobility and freeze in at lower temperatures producing a second glass transition. Unfortunately, we were not able to unambiguously determine whether the dielectric α′-relaxation is really characterized by isotropic molecular reorientation, as the α′ process only separates from the α-relaxation rather close to T_g and is thus outside the relevant time window, where NMR would be able to identify the motional mechanism in a straightforward manner. However, as the relaxation times of α′ hardly seem to depend on M-THF concentration, it is very likely that this situation can be improved by switching to a higher molecular weight polymer, so that both α- and α′-relaxations separate at significantly shorter times and α′ becomes accessible to NMR investigations. Such experiments are currently in progress.

Usually, in polymer mixtures time scale separation is rationalized in terms of self-concentration effects due to chain connectivity.[20] In our case, however, such considerations are difficult to apply, as both molecules are considerably smaller than the Kuhn length of about 8 monomer units for polystyrene.[79] Maybe, as the smaller molecules take part in both relaxations, our experimental findings can better be compared with the situation found for glass formers confined in porous media, where surface effects are known to occur: typically, a slow or immobilized layer of molecules is found close to the confining wall, whereas the mobility increases in the center of the pores, which may even lead to a bimodal distribution of relaxation times.[53−55] Thus, in the mixtures the larger molecules impose a slow but soft confinement on the small molecules when the system is above the upper T_g. Below the upper T_g the matrix is nonergodic and effects of hard confinement are expected, and indeed, the faster α′-relaxation follows an Arrhenius behavior in this temperature range. Whether there is a stronger, more Vogel−Fulcher-like temperature dependence of $\tau_{\alpha'}$ at higher temperatures cannot be decided so far as both α- and α′-relaxations merge above but rather close to T_g.

We also note here that concentration fluctuations, which are found to decay on the length and time scales associated with the photon correlation experiment, seem to have a stronger influence on the spectral broadening of the smaller component. This may indicate that different length scales of cooperative motion are relevant for each molecular species. However, it is also observed that the decay of concentration fluctuations interferes with the α-relaxation time scale around T_g, similar to observations made with XPCS on a comparable system.[16] If the decay of concentration fluctuations indicates the time scale of dynamic exchange present in the binary mixture, an intersection of both traces would imply a narrowing of the relaxation spectra at lower temperatures. This of course it not observed, so that dynamic exchange has to occur on an even longer time scale. In order to shed further light on this issue, two-dimensional NMR experiments will be required. Furthermore, concentration fluctuations in dynamically asymmetric binary mixtures are known to display aging effects in the crossover region close to T_g, and are observed to slow down as a function of waiting time, as indicated by recent XPCS experiments.[80] Thus, it is possible that an intersection of τ_α and τ_{CF} is only seen in the nonergodic regime, while in equilibrium $\tau_{CF} > \tau_\alpha$ holds, as is commonly assumed. Further experiments are required to elucidate this point.

In order to clarify the nature of the two secondary relaxations which are observed in the M-THF mixtures, we also included mixtures of THF in tristyrene in the discussion. Basically, all main and secondary relaxations appear in a very similar manner in both types of mixtures; in particular, the magnitude and temperature dependence of the time constants are either identical or very similar. Clearly, ^{2}H NMR experiments on deuterated THF in the mixture reveal that the β-process upon entering the NMR time window only has very slight effects on the spectra, indicating the β-relaxation only involves small-angle reorientation of the C$-^2$H bonds as is typical of a JG β-relaxation. The δ-relaxation, on the other hand, is related to considerably larger jump angles. Thus, the latter relaxation can be related to conformational changes of the nonrigid THF ring. This conclusion is well in accord with recent observations made in mixtures of benzophenone or various phthalates in oligostyrene, where the slower of the two secondary relaxations observed was identified as being a JG process, whereas the faster was ascribed to internal degrees of freedom of the dipolar component.[81]

When comparing the THF with the M-THF mixtures, the relaxation strength of the δ-process in the latter is considerably smaller than in the former, so that we conclude that the angle of dipolar reorientation is reduced and the large angles involved in conformational changes as expected from ab initio calculations and the simulation of the NMR spectra of THF in the mixture are greatly reduced due to the steric hindrance imposed by the additional methyl group so that only a certain internal motion of the THF ring remains in the M-THF systems. As is clear from the analysis of the dielectric data that the high-frequency wing in neat M-THF has to be identified with the β-relaxation in the corresponding mixtures, it thus turns out that the HF-wing represents the actual JG β-relaxation in pure M-THF, whereas the additional small δ-peak is due to internal degrees of freedom within the THF ring.

AUTHOR INFORMATION

Corresponding Author

*E-mail: thomas.blochowicz@physik.tu-darmstadt.de.

ACKNOWLEDGMENT

We are indebted to J. A. Sordo from Universidad de Oviedo, Spain, for kindly providing the Cartesian coordinates for the THF molecule in the S0, S1, and S2 configurations. Moreover, we gratefully acknowledge financial support by the Deutsche Forschungsgemeinschaft under grant no. BL 923/1.

REFERENCES

(1) Utracki, L. A. *Polymer alloys and blends: thermodynamics and rheology*; Hanser Verlag: München, Germany, 1989.

(2) Blochowicz, T.; Karle, C.; Kudlik, A.; Medick, P.; Roggatz, I.; Vogel, M.; Tschirwitz, C.; Wolber, J.; Senker, J.; Rössler, E. Molecular dynamics in binary organic glass formers. *J. Phys. Chem. B* **1999**, *103*, 4032.

(3) Colmenero, J.; Arbe, A. Segmental dynamics in miscible polymer blends: recent results and open questions. *Soft Matter* **2007**, *3*, 1474.

(4) Vogel, M.; Medick, P.; Rössler, E. Slow molecular dynamics in binary organic glass formers. *J. Mol. Liq.* **2000**, *86*, 103.

(5) Bingemann, D.; Wirth, N.; Gmeiner, J.; Rössler, E. A. Decoupled dynamics and quasi-logarithmic relaxation in the polymer-plasticizer

system poly(methyl methacrylate)/tri-m-cresyl phosphate studied with 2D NMR. *Macromolecules* **2007**, *40*, 5379.

(6) Gaikwad, A. N.; Wood, E. R.; Ngai, T.; Lodge, T. P. Two calorimetric glass transitions in miscible blends containing poly(ethylene oxide). *Macromolecules* **2008**, *41*, 2502.

(7) Lodge, T. P.; Wood, E. R.; Haley, J. C. Two calorimetric glass transitions do not necessarily indicate immiscibility: The case of PEO/PMMA. *J. Polym. Sci. B: Polym. Phys.* **2006**, *44*, 756.

(8) Miwa, Y.; Usami, K.; Yamamoto, K.; Sakaguchi, M.; Sakai, M.; Shimada, S. Direct detection of effective glass transitions in miscible polymer blends by temperaturemodulated differential scanning calorimetry. *Macromolecules* **2005**, *38*, 2355.

(9) Sakaguchi, T.; Taniguchi, N.; Urakawa, O.; Adachi, K. Calorimetric study of dynamical heterogeneity in blends of polyisoprene and poly(vinylethylene). *Macromolecules* **2005**, *38*, 422.

(10) Plazek, D. J.; Riande, E.; Markovitz, H.; Raghupathi, N. Concentration dependence of the visoelastic properties of polystyrene-tricresyl phosphate solutions. *J. Polym. Sci., Polym. Phys. Ed.* **1979**, *17*, 2189.

(11) Adachi, K.; Ishida, Y. Effect of diluent on molecular motion and glass transition in polymers. iv. the system poly(methyl acrylate)−toluene. *Polymer J.* **1979**, *11*, 233.

(12) Savin, D. A.; Larson, A. M.; Lodge, T. P. Effect of composition on the width of the calorimetric glass transition in polymersolvent and solvent-solvent mixtures. *J. Polym. Sci. B: Polym. Phys.* **2004**, *42*, 1137.

(13) Lipson, J. E. G.; Milner, S. T. Multiple glass transitions and local composition effects on polymer solvent mixtures. *J. Polym. Sci. Part B: Polym. Phys.* **2006**, *24*, 3528.

(14) Cangialosi, D.; Alegría, A.; Colmenero, J. Self-concentration effects on the dynamics of a polychlorinated biphenyl diluted in 1,4-polybutadiene. *J. Chem. Phys.* **2007**, *126*, 204904.

(15) Medick, P.; Vogel, M.; Rössler, E. Large angle jumps of small molecules in amorphous matrices analyzed by 2D exchange NMR. *J. Magn. Reson.* **2002**, *159*, 126.

(16) Schramm, S.; Blochowicz, T.; Gouirand, E.; Wipf, R.; Stühn, B.; Chushkin, Y. Concentration fluctuations in a binary glass former investigated by x-ray photon correlation spectroscopy. *J. Chem. Phys.* **2010**, *132*, 224505.

(17) Zetsche, A.; Fischer, E. W. Dielectric studies of the α-relaxation in miscible polymer blends and its relation to concentration fluctuations. *Acta Polym.* **1994**, *45*, 168.

(18) Kumar, S. K.; Colby, R. H.; Anastasiadis, S. H.; Fytas, G. Concentration fluctuation induced dynamic heterogeneities in polymer blends. *J. Chem. Phys.* **1996**, *105*, 3777.

(19) Kant, R.; Kumar, S. K. What length scales control the dynamics of miscible polymer blends? *Macromolecules* **2003**, *36*, 10087.

(20) Lodge, T. P.; McLeish, T. C. B. Selfconcentration and effective glass transition temperatures in polymer blends. *Macromolecules* **2000**, *33*, 5278.

(21) Chung, G.-C.; Kornfield, J. A.; Smith, S. D. Compositional dependence of the segmental dynamics in a miscible polymer blend. *Macromolecules* **1994**, *27*, 5729.

(22) Leroy, E.; Alegria, A.; Colmenero, J. Segmental Dynamics in Miscible Polymer Blends: Modeling the Combined Effects of Chain Connectivity and Concentration Fluctuations. *Macromolecules* **2003**, *36*, 7280.

(23) Shenogin, S.; Kant, R.; Colby, R. H.; Kumar, S. K. Dynamics of miscible polymer blends: Predicting the dielectric response. *Macromolecules* **2007**, *40*, 5767.

(24) Cangialosi, D.; Alegría, A.; Colmenero, J. Dielectric relaxation of polychlorinated biphenyl/toluene mixtures: Component dynamics. *J. Chem. Phys.* **2008**, *128*, 224508.

(25) Huang, D.; Simon, S. L.; McKenna, G. B Equilibrium heat capacity of the glassforming poly(α-methyl styrene) far below the kauzmann temperature: The case of the missing glass transition. *J. Chem. Phys.* **2003**, *119*, 3590.

(26) Dalle-Ferrier, C.; Simon, S.; Zheng, W.; Badrinarayanan, P.; Fennell, T.; Frick, B.; Zanotti, J. M.; Alba-Simionesco, C. Consequence of excess configurational entropy on fragility: the case of a polymer-oligomer blend. *Phys. Rev. Lett.* **2009**, *103*, 185702.

(27) Zheng, W.; Simon, S. L. The glass transition in athermal poly(α-methyl styrene)/oligomer blends. *J. Polym. Sci. B: Polym. Phys.* **2008**, *46*, 418.

(28) Bosse, J.; Thakur, J. S. Delocalization of small particles in a glassymatrix. *Phys. Rev. Lett.* **1987**, *95*, 998.

(29) Bosse, J.; Kaneko, Y. Self-diffusion in supercooled binary liquids. *Phys. Rev. Lett.* **1995**, *74*, 4023.

(30) Kaneko, Y.; Bosse, J. Dynamics of binary liquids near the glass transition: a modecoupling theory. *J. Non-Cryst. Solids* **1996**, *205*− *207*, 472.

(31) Voigtmann, T.; Horbach, J. Double transition scenario for anomalous diffusion in glass-forming mixtures. *Phys. Rev. Lett.* **2009**, *103*, 205901.

(32) Krakoviack, V. Liquid-glass transition of a fluid confined in a disordered porous matrix: A mode-coupling theory. *Phys. Rev. Lett.* **2005**, *94*, 065703.

(33) Krakoviack, V. Liquid−glass transition of confined fluids: insights from a modecoupling theory. *J. Phys.: Condens. Matter* **2005**, *17*, S3565–S3570.

(34) Krakoviack, V. Mode-coupling theory for the slow collective dynamics of fluids adsorbed in disordered porous media. *Phys. Rev. E* **2007**, *75*, 031503.

(35) Höfling, F.; Franosch, T.; Frey, E. Localization transition of the three-dimensional Lorentz model and continuum percolation. *Phys. Rev. Lett.* **2006**, *96*, 165901.

(36) Moreno, A. J.; Colmenero, J. Relaxation scenarios in a mixture of large and small spheres: Dependence on the size disparity. *J. Chem. Phys.* **2006**, *125*, 164507.

(37) Blochowicz, T.; Rössler, E. Beta relaxation versus high frequency wing in the dielectric spectra of a binary molecular glass former. *Phys. Rev. Lett.* **2004**, *92*, 225701.

(38) Capaccioli, S.; Kessairi, K.; Prevosto, D.; Lucchesia, M.; Ngai, K. L. Genuine Johari−Goldstein β-relaxations in glassforming binary mixtures. *J. Non-Cryst. Solids* **2006**, *352*, 4643.

(39) Qi, F.; El Goresy, T.; Böhmer, R.; Döss, A.; Diezemann, G.; Hinze, G.; Sillescu, H.; Blochowicz, T.; Gainaru, C.; Rössler, E. A.; Zimmermann, H. Nuclear magnetic resonance and dielectric spectroscopy of a simple supercooled liquid: 2-methyl tetrahydrofuran. *J. Chem. Phys.* **2003**, *118*, 7431.

(40) Schmidt-Rohr, K.; Spiess, H. W. *Multidimensional Solid-State NMR and Polymers*; Academic Press: London, 1994.

(41) Blochowicz, T.; Tschirwitz, C.; Benkhof, S.; Rössler, E. A. Susceptibility functions for slow relaxation processes in supercooled liquids and the search for universal relaxation patterns. *J. Chem. Phys.* **2003**, *118*, 7544.

(42) Blochowicz, T.; Brodin, A.; Rössler, E. A. Evolution of the dynamic susceptibility in supercooled liquids and glasses. *Adv. Chem. Phys.* **2006**, *133*, 127.

(43) Glasstone, S.; Laidler, K. J.; Eyring, H. *The Theory of Rate Processes*; McGraw Hill: New York, 1941.

(44) Kudlik, A.; Tschirwitz, C.; Blochowicz, T.; Benkhof, S.; Rössler, E. Slow secondary relaxation in simple glass formers. *J. Non- Cryst. Solids* **1998**, *235*−*237*, 406.

(45) Böttcher, C. J. F.; Bordewijk, P. *Theory of Electric Polarization II: Dielectrics in time dependent fields*; Elsevier: Amsterdam, 1978.

(46) Floudas, G.; Steffen, W.; Fischer, E. W.; Brown, W. Solvent and polymer dynamics in concentrated polystyrene/toluene solutions. *J. Chem. Phys.* **1993**, *99*, 695.

(47) Cangialosi, D.; Schwartz, G. A.; Alegría, A.; Colmenero, J. Combining configurational entropy and self-concentration to describe the component dynamics in miscible polymer blends. *J. Chem. Phys.* **2005**, *123*, 144908.

(48) Vogel, H. Das Temperaturabhängigkeitsgesetz der Viskosität von Flüssigkeiten. *Phys. Z.* **1921**, *22*, 645.

(49) Fulcher, G. S. Analysis of recent measurements of the viscosity of glasses. *J. Am. Ceram. Soc.* **1925**, *8*, 339.

(50) Tammann, G.; Hesse, W. Die Abhängigkeit der Viskosität von der Temperatur bei unterkühlten Flüssigkeiten. *Z. Anorg. Allg. Chem.* **1926**, *156*, 245.
(51) Hodge, I. M. Enthalpy relaxation and recovery in amorphous materials. *J. Non-Cryst. Solids* **1994**, *169*, 211.
(52) Vogel, M.; Rössler, E. Slow β-process in simple organic glass formers studied by one- and two-dimensional 2H nuclear magnetic resonance I/II. *J. Chem. Phys.* **2001**, *114*, 5802; *J. Chem. Phys.* **2001**, *115*, 10883.
(53) Kremer, F. Molecular dynamics in confining space. In *Broadband Dielectric Spectroscopy*; Kremer, F., Schönhals, A., Eds.; Springer: Berlin, 2003; p 171.
(54) Gradmann, S.; Medick, P.; Rössler, E. A. Glassy dynamics in nanoconfinement as revealed by 31P NMR. *J. Phys. Chem. B* **2009**, *113*, 8443–8445.
(55) Scheidler, P.; Kob, W.; Binder, K. The relaxation dynamics of a simple glass former confined in a pore. *Europhys. Lett.* **2000**, *52*, 277.
(56) Johari, G. P.; Goldstein, M. Viscous liquids and the glass transition II: Secondary relaxations in glasses of rigid molecules. *J. Chem. Phys.* **1970**, *53*, 2372.
(57) Vogel, M.; Tschirwitz, C.; Schneider, G.; Koplin, C.; Medick, P.; Rössler, E. A 2H NMR and dielectric spectroscopy study on the slow β-process in organic glass formers. *J. Non-Cryst. Solids* **2002**, *307*−*310*, 326.
(58) Ngai, K. L.; Paluch, M. Classification of secondary relaxation in glass-formers based on dynamic properties. *J. Chem. Phys.* **2004**, *120*, 857.
(59) Berne, B. J.; Pecora, R. *Dynamic Light Scattering*; Dover Publications Inc.: Mineola, NY, 2000.
(60) Blochowicz, T.; Kudlik, A.; Benkhof, S.; Senker, J.; Rössler, E.; Hinze, G. The spectral density in simple organic glassformers: Comparison of dielectric and spin-lattice relaxation. *J. Chem. Phys.* **1999**, *110*, 12011.
(61) Salaniwal, S.; Kant, R.; Colby, R. H.; Kumar, S. K. Computer simulations of local concentration variations in miscible polymer blends. *Macromolecules* **2002**, *35*, 9211–9218.
(62) Pake, G. E. Nuclear resonance absorption in hydrated crystals: Fine structure of the proton line. *J. Chem. Phys.* **1948**, *16*, 327.
(63) Lusceac, S. "Study of relaxation processes in simple glass formers by means of 2H NMR spectroscopy"; Ph.D. thesis, University of Bayreuth, Bayreuth, Germany, 2006.
(64) Williams, G.; Watts, D. C. Nonsymmetrical dielectric relaxation behaviour arising from a simple empirical decay function. *Trans. Faraday Soc.* **1970**, *66*, 80.
(65) Bloembergen, N.; Purcell, E. M.; Pound, R. V. Relaxation effects in nuclear magnetic resonance absorption. *Phys. Rev.* **1948**, *73*, 679.
(66) Abragam, A. *Principles of Nuclear Magnetism*; Clarendon Press: Oxford, UK, 1961.
(67) Vogel, M.; Medick, P.; Rössler, E. A. Secondary relaxation processes in molecular glasses studied by nuclear magnetic resonance spectroscopy. *Annu. Rep. NMR Spectrosc.* **2005**, *56*, 231.
(68) Lusceac, S. A.; Gainaru, C.; Koplin, C.; Medick, P; Rössler, E. A. Secondary relaxation processes in polybutadiene studied by 2H nuclear magnetic resonance and highprecision dielectric spectroscopy. *Macromolecules* **2005**, *38*, 5625.
(69) Davidson, D. W.; Garg, S. K.; Ripmeester, J. A. NMR behavior of the clathrate hydrate of tetrahydrofuran. II. deuterium measurements. *J. Magn. Reson.* **1978**, *31*, 399.
(70) Meirovitch, E.; Freed, J. H. Slow motional NMR lineshapes for very anisotropic diffusion:I=1-nuclei. *Chem. Phys. Lett.* **1979**, *64*, 311.
(71) Nowaczyk, A.; Geil, B.; Schildmann, S.; Böhmer, R. Guest motion in tetrahydrofuran clathrate hydrate studied by deuteron nuclear magnetic resonance. *Phys. Rev. B* **2009**, *80*, 144303.
(72) Rayón, V. M.; Sordo, J. A. Pseudorotation motion in tetrahydrofuran: An ab initio study. *J. Chem. Phys.* **2005**, *122*, 204303.
(73) Hinze, G. Geometry and time scale of the rotational dynamics in supercooled toluene. *Phys. Rev. E* **1998**, *57*, 2010.
(74) Vogel, M.; Rössler, E. Effects of various types of molecular dynamics on 1D and 2D 2H NMR studied by random walk simulations. *J. Magn. Reson.* **2000**, *147*, 43.
(75) Böhmer, R.; Diezemann, G.; Hinze, G.; Rössler, E. Dynamics of supercooled liquids and glassy solids. *Prog. NMR Spectrosc.* **2001**, *39*, 191.
(76) Medick, P.; Blochowicz, T.; Vogel, M.; Rössler, E. Comparing the dynamical heterogeneities in binary glass formers and in a glass former embedded in a zeolite - a ^{2}H NMR study. *J. Non-Cryst. Solids* **2002**, *307*, 565.
(77) Gedat, E.; Schreiber, A.; Albrecht, J.; Emmler, T.; Shenderovich, I.; Findenegg, G. H.; Limbach, H.-H.; Buntkowsky, G. ^{2}H-solid-state NMR study of benzene-d_6 confined in mesoporous silica SBA-15. *J. Phys. Chem. B* **2002**, *106*, 1977.
(78) Lusceac, S. A.; Koplin, C.; Medick, P.; Vogel, M.; Brodie-Linder, N.; LeQuellec, C.; Alba-Simionesco, C.; Rössler, E. A. Type A versus type B glass formers: NMR relaxation in bulk and confining geometry. *J. Phys. Chem. B* **2004**, *108*, 16601.
(79) Pedersen, J. S.; Schurtenberger, P. Static properties of polystyrene in semidilute solutions: A comparison of monte carlo simulation and small-angle neutron scattering results. *Eur. Phys. Lett.* **1999**, *45*, 666.
(80) Schramm, S.; Blochowicz, T.; Gouirand, E.; Chushkin, Y.; Stühn, B. Manuscript in preparation, 2010.
(81) Capaccioli, S.; Thayyil, M. S.; Ngai, K. L. Critical issues of current research on the dynamics leading to glass transition. *J. Phys. Chem. B* **2008**, *112*, 16035.
(82) Zhao, M.; Jin, L.; Chen, B.; Ding, Y.; Ma, H.; Chen, D. Afterpulsing and its correction in fluorescence correlation spectroscopy experiments. *Appl. Opt.* **2003**, *42*, 4031.
(83) A detailed analysis of the temperature dependence of $\Delta\varepsilon_\alpha$ and $\Delta\varepsilon_{\alpha'}$ will be presented for a similar and slightly more favorable system containing a longer chain polystyrene in a following publication.
(84) Since the depolarized correlation functions due to the low overall scattering intensity were not recorded in pseudo-cross-correlation mode but rather with a single avalanche photodiode, the correlation functions were corrected for afterpulsing effects at short times according to the method suggested by Zhao et al.[82]